

# Photoelectrochemical characterization of amorphous anodic films on Ti–6at.%Si

F. Di Quarto<sup>a</sup>, F. Di Franco<sup>a</sup>, C. Monarca<sup>a</sup>, M. Santamaria<sup>a,\*</sup>, H. Habazaki<sup>b</sup>

<sup>a</sup> Electrochemical Material Science Laboratory, DICAM-Università di Palermo, Viale delle Scienze 90128, Palermo, Italy

<sup>b</sup> Graduate School of Engineering, Hokkaido University, Sapporo 060-8628, Japan

## ARTICLE INFO

### Article history:

Received 19 December 2012

Received in revised form 21 January 2013

Accepted 23 January 2013

Available online 31 January 2013

### Keywords:

Anodic films

Amorphous TiO<sub>2</sub>

Si–TiO<sub>2</sub>

Band gap

Flat band potential

## ABSTRACT

The solid state properties of anodic films grown galvanostatically on sputtering-deposited Ti–6at.%Si alloys were studied as a function of the formation voltage (5–40 V). From the photocurrent spectra a band gap of ~3.4 eV was estimated for all the investigated thicknesses, which is almost coincident with the value measured for amorphous TiO<sub>2</sub>. The photocharacteristics allowed to estimate the flat band potential of the films, which resulted to be more anodic for thicker layers and allowed to evidence a change from n-type semiconducting material to insulator by increasing the formation voltage. A dielectric constant of ~31 was estimated by differential capacitance measurements. The dependence of photocurrent on electrode potential was studied in the frame of Onsager–Braun theory, which allows to evidence the influence of the initial recombination on the photocurrent yield for amorphous material.

© 2013 Elsevier Ltd. All rights reserved.

## 1. Introduction

The occurrence of crystallization phenomena during the anodizing of valve metals and/or when high electric fields are applied across already formed anodic films is an important issue for their use as dielectric in the electronic industry. A dense and flaw-free barrier oxide must be formed to work as a dielectric in capacitor or in memristor [1,2].

Anodic titanium oxide has attracted much attention in micro- and nano-electronics due the high dielectric constant of TiO<sub>2</sub> (ranging between 24 and 53 [3–6]). However, anodic TiO<sub>2</sub> films develop with a high population density of flaws on high purity titanium in aqueous electrolytes. Thus, anodic titanium oxide-based capacitors have not been realized practically despite the large permittivity of the oxide with respect to anodic aluminium oxide ( $\epsilon_{\text{ox}} = 10$ ) and tantalum oxide ( $\epsilon_{\text{ox}} = 27$ ), currently used in commercial electrolytic capacitors.

Previous works [7] have shown that the development of flaws in anodic TiO<sub>2</sub> is associated with crystallization of the film during anodizing. The crystalline regions are reported to enable oxygen evolution, due to their increased electronic conductivity with respect to the amorphous counterpart. The consequent increased pressure can bring to film breakdown, which is detrimental for capacitors.

Several strategies have been proposed in the literature to hinder or delay the onset of crystallization during anodizing of TiO<sub>2</sub>.

It is widely accepted that the onset of crystallization is delayed by the incorporation of foreign species inside the oxide [7–9]. These species can come from the electrolyte and, according to their relative migration rate compared to that of the ions involved in the oxide formation (i.e. Ti<sup>4+</sup> and O<sup>2-</sup>), they contribute to keep amorphous the outer part of the anodic film.

But foreign species can be incorporated into the anodic films by alloying to titanium small amount of another element, namely silicon. The occurrence of amorphous to crystalline transition during the anodizing of Ti and Ti–Si alloys has been extensively studied in Refs. [8,9] by ex situ optical techniques, like transmission electron microscopy of ultramicrotomed sections, which allowed to well characterize the structural features of the anodic films as a function of the anodizing conditions (alloy composition and ageing, anodizing electrolyte). Moreover, this transition has been related to the film composition by both ex situ Rutherford back scattering (RBS) and glow discharge optical emission spectroscopy (GDOES), which allowed to evidence the presence of Si in the inner part of the anodic films corresponding to the 40% of the whole film thickness. These experimental findings unambiguously demonstrate that Si has an effective role in delaying the crystallization and breakdown of TiO<sub>2</sub>. It remains to explain the effect of Si on the solid state properties of anodic films on Ti–Si alloys. Thus, this work is focused on the physico-chemical characterization of anodic films on sputtering-deposited Ti–6at.%Si alloys as a function of their thickness (i.e. formation voltage). Photocurrent spectroscopy allowed to estimate the band gap, flat band potential and conductivity type of the investigated films, while their dielectric constant was estimated by differential capacitance measurements. The dependence of the photocurrent on the electric field and on the photon energy is

\* Corresponding author.

E-mail address: [monica.santamaria@unipa.it](mailto:monica.santamaria@unipa.it) (M. Santamaria).

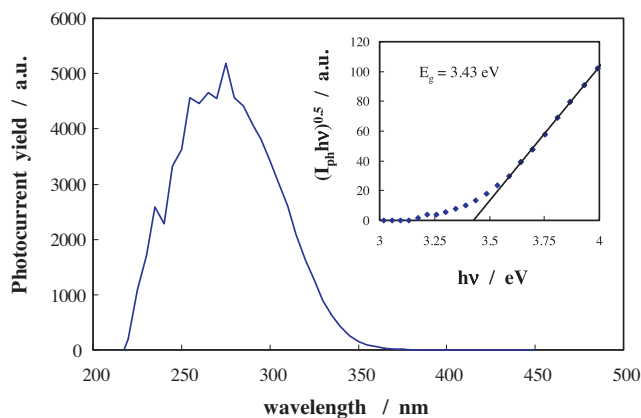


**Fig. 1.** Photocurrent spectrum relating to anodic films grown to  $U_F = 5\text{V}$  in  $1\text{ mol dm}^{-3}\text{ H}_3\text{PO}_4$  at  $5\text{ mA cm}^{-2}$  on Ti–6at.%Si alloy, recorded by polarizing the electrodes at 3V vs Ag/AgCl in  $0.1\text{ mol dm}^{-3}$  ABE. Inset: Band gap estimate by assuming non direct optical transitions.

studied taking into account the amorphous structure of the investigated films, and modelled on the basis of the Braun–Onsager theory.

## 2. Experimental

Ti–6%Si alloy was prepared by co-sputtering of 99.5% titanium and 99.999% silicon using a dc magnetron sputtering method. The alloy was deposited, as a layer about 200 nm thick, on glass substrates [8,9].

The deposited layers were anodized to several final voltages (from 5 to 40V) at  $5\text{ mA cm}^{-2}$  in phosphoric acid at room temperature.

The experimental set-up for the photo-electrochemical measurements has been described elsewhere [10]. A 450W UV–vis xenon lamp coupled with a monochromator, allows irradiation of the specimen through a quartz window. A two-phase lock-in amplifier, with a mechanical chopper, enables separation of the photocurrent from the total current in the cell. The photocurrent spectra are corrected for the relative photon efficiency of the light source at each wavelength, so that the photocurrent yield in arbitrary current units is represented on the y-axis.

The photoelectrochemical experiments were carried out in  $1\text{ mol dm}^{-3}\text{ H}_3\text{PO}_4$  and  $0.1\text{ mol dm}^{-3}\text{ (NH}_4)_2\text{B}_4\text{O}_7$  (ABE) aqueous solutions.

A silver–chloride electrode (0V vs Ag/AgCl = 0.197V vs SHE) was employed as reference electrode for all the electrochemical and photoelectrochemical experiments.

Differential capacitance curves were recorded in  $1\text{ mol dm}^{-3}\text{ H}_3\text{PO}_4$  solution with  $v_{a.c.} = 10\text{ mV}$  by using a Parstat 2263 (PAR), connected to a computer for the data acquisition. For all the experiments, a Pt net having a very high surface area was used as counter electrode and a silver/silver chloride electrode was employed as reference electrode.

## 3. Results

### 3.1. Photoelectrochemical results

Photocurrent spectra were recorded for anodic films grown on Ti–6at.%Si as a function of the formation voltage (i.e. thickness). In Fig. 1 we report the photocurrent yield,  $I_{ph}$  (photocurrent corrected for the efficiency of the lamp–monochromator system, see Ref. [10]) as a function of the irradiating wavelength relating to a 5V anodic film, recorded by polarizing the electrode at 3V (SSC). Considering that  $I_{ph}$  can be assumed proportional to the light absorption

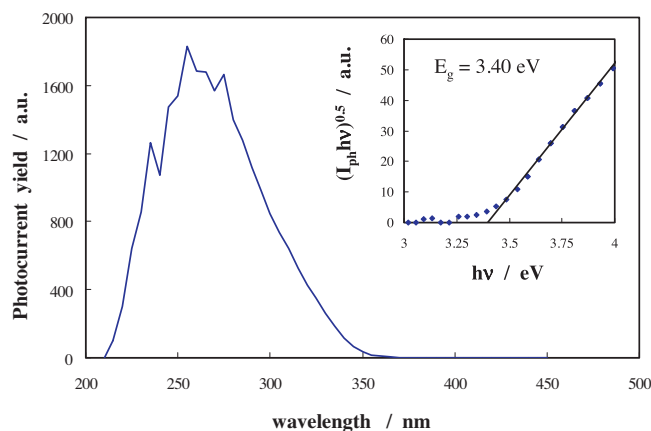


**Fig. 2.** Photocurrent spectrum relating to anodic film grown to  $U_F = 40\text{V}$  in  $1\text{ mol dm}^{-3}\text{ H}_3\text{PO}_4$  at  $5\text{ mA cm}^{-2}$  on Ti–6at.%Si alloy, recorded by polarizing the electrodes at 5V vs Ag/AgCl in  $0.1\text{ mol dm}^{-3}$  ABE. Inset: Band gap estimate by assuming non direct optical transitions.

coefficient, for a photon energy in the vicinity of the band gap, the following equation holds:

$$(I_{ph}hv)^n \propto (hv - E_g) \quad (1)$$

where  $hv$  is the photon energy,  $E_g$  is the optical band gap and the exponent  $n$  is 0.5 for indirect (non-direct for amorphous materials) optical transitions [11]. As shown in the inset, an optical band gap of 3.43 eV can be estimated for this oxide by extrapolating to zero the  $(I_{ph}hv)^{0.5}$  vs  $hv$  plot.

Not appreciable differences were evidenced in the photocurrent spectra relating to thicker films for formation voltages  $\leq 40\text{V}$  (see Fig. 2).

If we anodize silicon free titanium in the same conditions ( $5\text{ mA cm}^{-2}$  in  $\text{H}_3\text{PO}_4$ ) the optical band gap is  $\sim 3.40\text{ eV}$  for formation voltage  $\leq 10\text{V}$  (see Fig. 3a), while  $E_g = 3.30\text{ eV}$  can be estimated for 20V and 40V anodic film (see Fig. 3b). An appreciable tailing in the photocurrent spectra can be observed due to optical transitions at energy lower than the band gap of the oxide, which interests a wider wavelengths range for thick films (see Fig. 3b).

It is interesting to stress that the measured band gap values for anodic films grown on both Ti and Ti–6at.%Si are higher than those reported for crystalline  $\text{TiO}_2$  (i.e. 3.2 eV for anatase and 3.05 eV for rutile, see Ref. [5]). As discussed in previous works [5,10], this difference can be attributed to the amorphous nature of the layers and, of relevance, it keeps constant as a function of the film thickness for Si containing films, while decreases for those grown on Ti.

In Fig. 4a and b we report the photocurrent vs potential curves (photocharacteristics), relating to the 5V anodic films on Ti–6at.%Si and Ti, recorded at several constant irradiating wavelengths. In both cases the photocurrent decreases by decreasing the polarizing voltage, as expected for n-type SC materials, and goes to zero at  $\sim -0.6\text{V}$  (vs Ag/AgCl). The zero photocurrent potential can be assumed as a proxy of the flat band potential [10]. Moreover, in both cases the transport equations usually employed to describe the behaviour of crystalline SC, based on the Gärtner–Butler model, seem to be not adequate, as evidenced, many years ago, in a previous paper on the photoelectrochemical behaviour of amorphous anodic film on W [12]. This model predicts the absence of any influence of the photon energy on the shape of the photocharacteristics, as well as a linear dependence of  $I_{ph}^2$  on electrode potential, provided that surface and space charge recombination phenomena are negligible, as usually occurs at high band bending as long as the space charge region width (or film thickness for insulating materials) is much smaller than the light absorption length,  $\alpha^{-1}$ . For amorphous materials we have to take into account the possible presence

Download English Version:

<https://daneshyari.com/en/article/6615687>

Download Persian Version:

<https://daneshyari.com/article/6615687>

[Daneshyari.com](https://daneshyari.com)